

Mars Rover Rocker-Bogie Comparative Differential Study

Matthew Woodall, Gunnar Baechler, Iman Salehinia, Nicholas A. Pohlman

Department of Mechanical Engineering, Northern Illinois University, DeKalb, Illinois, United States

ABSTRACT: Rover vehicles can accomplish extreme terrain traversal through implementation of a Rocker-Bogie suspension mechanism. Rocker-Bogie mechanisms include independent pivoting linkages on either side of the rover connected through a differential system that keeps the chassis level. This study's purpose is to perform a comparative analysis on the performance differences between two types of differential systems for a Rocker-Bogie suspension: a differential gearbox and a differential rod. The performance parameters analyzed were the pitch angle, roll angle, and resulting play in the pitch referred to as delta at increasing inclinations of the rocker linkage. These parameters were compared to idealized values from theoretical calculations. Hypothesis testing was applied to show there were statistically significant differences between the collected angle values of each differential system to distinguish performance of one system from the other. There was ample evidence to show a significant performance difference between the two systems in relation to resulting pitch angles and pitch delta, however there was not enough evidence to show performance differences in the roll angle except at extreme inclinations. With a 99% confidence level, the differential rod's performance was shown to be better than the differential gearbox via the Picus Number, a derived performance metric value for Rocker-Bogie differentials. The evidence of better performance led to further analysis and the implementation of the differential rod system on the NIU Mars Rover Team's competition Mars rover, PicusMartius.

I. INTRODUCTION

Surface exploration of Mars was first achieved by the USA's Sojourner as part of NASA's Pathfinder Mission in 1997. Sojourner featured a Rocker-Bogie suspension system to permit the ability to traverse the expected rough terrain of Mars [1]. The Rocker-Bogie suspension is also implemented on the current NASA Mars rover, Curiosity, indicating that this mechanism is an effective suspension system for rovers.

The Rocker-Bogie mechanism, as the name suggests, is comprised of two major components: the rocker and the bogie (Fig. 1). The rocker is the large link that is the direct connection to the chassis of the rover via the differential shaft at the joint indicated in Fig. 1 and allows the rover to "rock" up and down to balance the weight distribution on the wheels [2]. The bogie is the smaller link that freely rotates about the end of one end of the rocker linkages via the Free Pivot Joint. The bogie serves as a load-bearing device and aids in the distribution of the weight onto all six wheels as the rover navigates different landscape.

A differential is a device that transmits torque and rotation from one coordinate plane to another normal to the first. Depending on the system, differentials may have a range of combinations of inputs and outputs leading to a versatile list of possible applications. The most common application for a differential is in automobiles where there is one input (plane pointing in the vehicle direction of motion) and two outputs allowing the inner and outer drive wheels (in the plane parallel to the motion) to travel at different speeds in order to cover the different arc lengths needed to turn a corner in the same amount of time [3]. In the case of the Rocker-Bogie, there are two inputs and one output given each rocker linkage has restricted free rotation due to the rocker-bogie system's contact with the ground.

The differential inputs come from each rocker linkage's direct connection to the drive shaft. From the side-view shown in Fig. 1, the drive shaft can be seen to run along the x-axis of the rover making each rocker linkage rotate in the ZY plane. The differential transfers this rotation in ZY to rotation in XY. Since there is a rocker linkage on each side of the rover, the rotation of one linkage ZY drives an equal and opposite rotation of the other linkage in ZY given the differentials translation through XY. The bogie linkage has free rotation about one end of the rocker allowing it to respond in a way that evenly distributes weight on the three wheels in the rocker-bogie system on the one side. This also drives the equal and

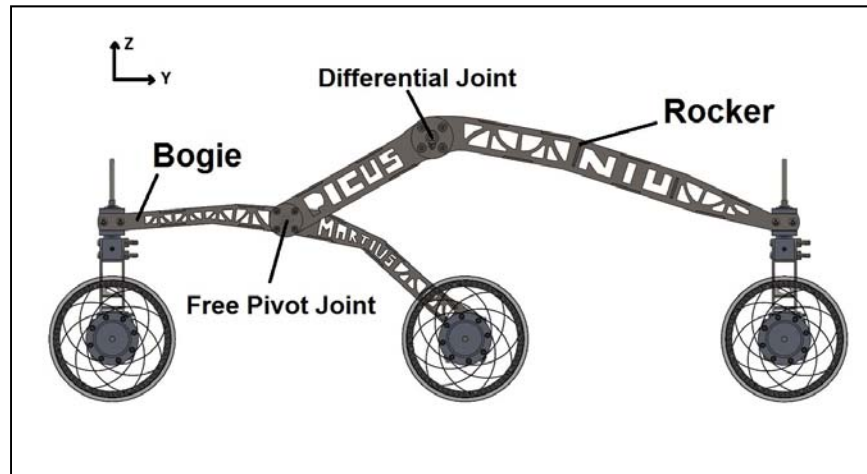


Figure 1: Solidworks® render side-view of the rocker-bogie and wheel assembly mechanisms used on the NIU Mars Rover Team rover, PicusMartius.

opposite rotation to the other linkage allowing gravity to drive the suspension aspect of the system forcing all six wheels to stay in contact with the ground even if one of the wheels is on a different level of terrain.

This work investigates the implementation of two differentials types, i.e. (i) a bevel-gear system and (ii) a rod mechanism consisting of a series of levers and a pivot. Though most analyses of the rocker-bogie mention the type of differential used, few mention the design justification decision process behind the selection. The California State – Fullerton Mars Rover Team’s 2014 final report [4] described a differential gearbox or rod as possible design solutions. The team stated that they chose to use the differential gearbox citing vibration issues with the rod system, however the method of determining this was never stated and the type of vibration issues were never defined. Considering no described methodology in choosing the differential system type, this work developed a way to analyze differential effectiveness and choose a system based on quantitative reasoning was developed. The design of each system analyzed with this method is specific to the NIU Mars Rover Team’s rover, PicusMartius.

II. DESIGN DETAILS

Design of Differential Gearbox

The chassis dimensions were predetermined to be width and length of 18” x 24” (457.2mm x 609.6mm) and the height based off the size of the differential gearbox driven by the minimal gear size. The height is limited by the gearbox because the minimal gear containment requirements are static while the rest of the components that will live in the chassis can be placed as needed. Sizing of the miter gears used in the differential was based upon the allowable contact stress and the allowable bending stress derived from the American Gear Manufacturer’s Association (AGMA) equation factors and standards offered in [5]. Equations (1) and (2) are the contact stress (s_c) and bending stress (s_t) in U.S. customary units, respectively. The equations’ parameter definitions are listed in Table 1.

$$s_c = C_p \left(\frac{W^t}{F_d p I} K_o K_v K_m C_s C_{xc} \right)^{1/2} \tag{1}$$

$$s_t = \frac{W^t}{F} P_d K_o K_v \frac{K_s K_m}{K_x J} \tag{2}$$

Table 1: Contact and bending stress equation parameters.

W^t	Tangential or transmitted load that would occur if all forces were concentrated at the midpoint of the tooth
F	Net Face Width
I	Pitting Resistance Geometry Factor
J	Bending Strength Geometry Factor
d_p	Pitch Diameter
P_d	Diametral Pitch
C_p	Elastic Coefficient for Pitting Resistance
C_s	Size Factor for Pitting Resistance
C_{xc}	Crowning Factor for Pitting
K_o	Overload Factor
K_v	Dynamic Factor
K_m	Load-Distribution Factor
K_s	Size Factor for Bending
K_x	Lengthwise Curvature Factor for Bending Strength

The transmitted load (W^t) can be calculated by the applied torque (T) and the pitch radius (r_{av}) shown in Eq. (3).

$$W^t = \frac{T}{r_{av}} \quad (3)$$

Resulting pitch diameters and thus the resulting pitch radii can be calculated through iterations of different number of teeth (N_t) and diametral pitches of a gear shown in Eq. (4). The transmitted load can be represented as a function of the pitch diameter shown in Eq. (5).

$$2r_{av} = d_p = \frac{N_t}{P_d} \quad (4)$$

$$W^t = \frac{2T}{d_p} \quad (5)$$

The resulting torque acting on the driving miter gears was approximated to be $T = 385$ lb-in (43.5 Nm) based on static relations of the manipulation system's allocated weight and electrical components' allocated weight in spatial relation to the gearbox shaft. With the estimated torque, the transmitted load was calculated for the varying diametral pitches to determine expected stresses for the different sized gears. The allocated weight for the manipulation system was 30 lbs (13.61 kg) and the allocated weight for the electronics was 10 lbs (4.54 kg).

The resulting values for the AGMA factors were derived based upon the usage of steel miter gears for a 3-miter differential setup and a 4-miter differential setup. The different setups would change some of the AGMA factors due to the non-driving gear being cantilevered or simply supported. It was also assumed that the steel miter gears were of AGMA Grade 2 and case hardened, thus the allowable contact stress was calculated as $s_{ac} = 225000$ psi (1.55 GPa) and the allowable bending stress was $s_{at} = 35000$ psi (0.24 GPa) [5]. Various numbers of gear teeth and diametral pitch combinations for a range of pitch diameters from 0.5" to 6" (12.7 mm to 152.4 mm) were iterated to find a combination that would result in a gear's resultant contact and bending stresses that satisfy the allowable contact and bending stress of the desired gear for purchase.

Fig. 2 shows the resulting contact and bending stresses for a steel miter gear with the estimated torque applied at various pitch diameters compared to the allowable contact and bending stresses. The 4-miter setup was chosen for implementation with 2.00" (50.8 mm) pitch diameters over the 3-miter setup with 2.60" (66.04 mm) pitch diameters due to cost, availability, and minimizing gearbox dimensions. The size of the gearbox was determined from the length needed to create proper mates for the miter gears seen in product specifications in Fig. 3. The distance from center of one miter gear to

the end of the mated gear is seen to be 2.00” (50.8 mm) making the internal dimensions of the gearbox to be a 4.00” x 4.00” (101.6 mm x 101.6 mm) box to properly mate a 4-miter setup.

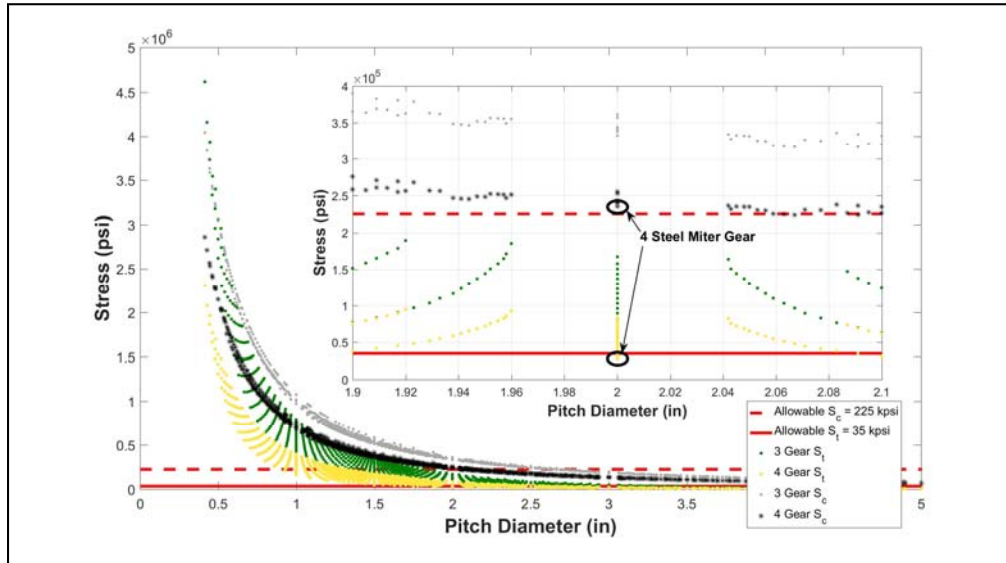


Figure 2: Resulting pitch diameter from iterating the number of teeth and diametral pitch values compared to the associated contact and bending stresses for 3-miter and 4-miter differential setups.

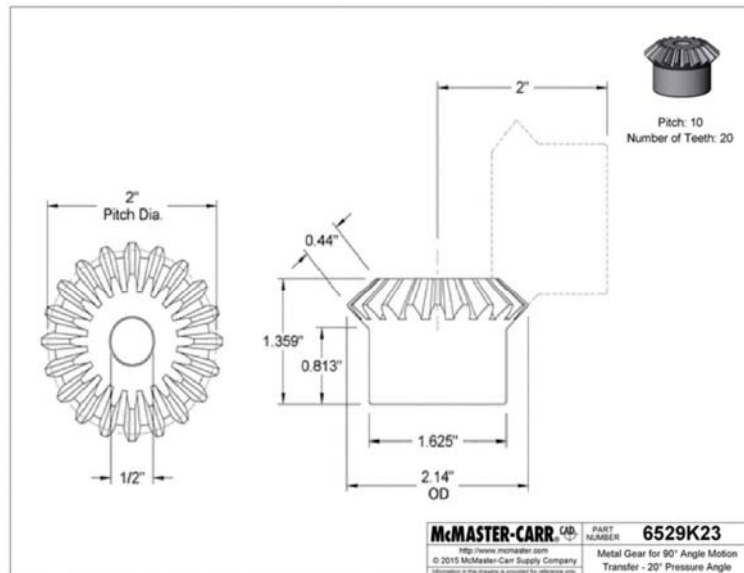


Figure 3: Drawing of 2” (50.8 mm) Pitch Diameter Miter Gear purchased from McMaster-Carr indicating the mate dimensions and overall hub diameters used

Using 0.25” (6.35 mm) thick aluminum to construct the box, the height of the chassis equated the external dimensions of the gearbox making the height 4.25” (107.95 mm) given an open top. Fig. 4 displays the highlighted gearbox within the chassis and the overall height of the chassis matches the size of the gearbox. The gearbox was placed off-center to the front of the chassis to compensate for the expected larger amount of weight on the back side where the manipulator would be mounted. This front off-center approach was designed to get the centroid of the resulting moments as close to the center of the gearbox’s drive shafts as possible.

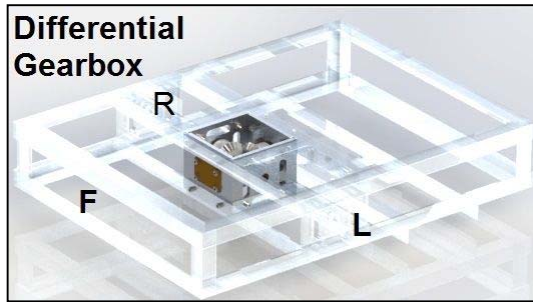


Figure 4: SolidWorks® render of the differential gearbox located inside of the chassis with the front, left, and right sides indicated. Note how the height of the chassis reflects the height of the gearbox.

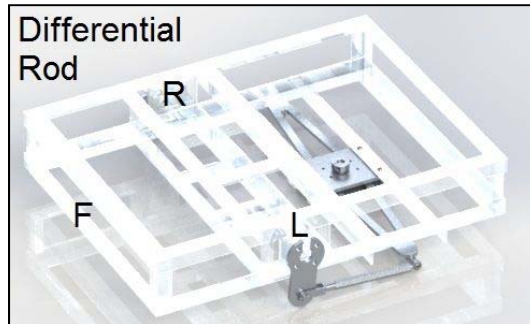


Figure 5: SolidWorks® render of the differential rod system mounted underneath the chassis to allow for mounting and open space on top of the chassis.

Design of Differential Rod

The differential rod replicates a gear mesh’s resulting rotation transfer of the rocker via a series of linkages that connect the left and right rocker drive shafts with a pivot shaft whose rotation is perpendicular to the rocker drive shafts beneath the chassis (see Fig. 5).

The suspension system was designed to allow rotation of the rocker $\pm 60^\circ$ from the ground about the drive shaft. This rotation is translated into the rod system by a link that connects to the rocker shown in Fig. 6. This linkage drives the pivot link shown in Fig. 7 from a connection at the pin joint (A) (see Fig. 6) to the end of the pivot link. The pin joint (A)’s range of motion was designed to stay below the chassis during operation. Designing the rod system to operate below the chassis provided the necessary space for the manipulator, science task components, and electronic mounting. The links described in Fig. 6 and Fig. 7 can be seen with connections in the full system shown in Fig. 5.

III. EXPERIMENTAL PROCEDURE

Testing was conducted via moving the rocker-bogie to simulate uneven terrain. The effectiveness of each differential system was evaluated. The orientation of the rover was determined via the pitch angle (θ) and the roll angle (ϕ) shown in Fig. 8a. At any point in time, the pitch angle exists within a range of angles determined by the pitch max and min of each measurement referred to as delta (Δ). This delta range of pitch angles can be thought of as the “wobble” or “play” in the pitch and is key in determining the effectiveness of the differential system’s ability to keep the chassis stable. The delta at each pitch angle can be calculated using Eq. (6).

$$\Delta_i = \theta_{i_{max}} - \theta_{i_{min}} \text{ for measurement } i \tag{6}$$

Three measurement tools were utilized to collect data of the roll angle, pitch angle, pitch max, pitch min, and rocker inclination angle. The roll angle was measured using the Mitutoyo digital protractor while the pitch, pitch max, and pitch min were measured using the SmartTool Angle Finder. These two instruments went through their respective calibration methods aligning with respect to the plane of the table. The Angle Finder was attached to the top of the chassis using double-sided tape, while the digital protractor was attached in a similar fashion to the front of the chassis. A magnetic protractor was attached to the end of the drive shaft on the rocker linkage to measure the rocker inclination angle, as seen in Fig. 8b.

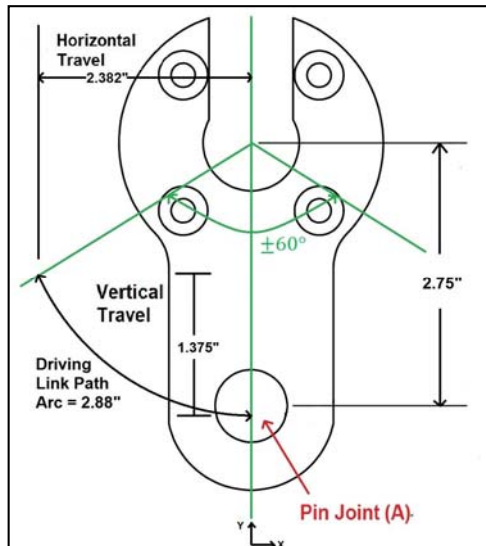


Figure 6: Differential Rod Driving Link. The four mount points connect directly to each rocker around the drive shaft. The pin joint (A) allows for any rotation about the drive shaft to be translated to the driving link path arc. The pivot link and this driving link are connected by a rod to translate the driving link rotation to pivot link rotation.

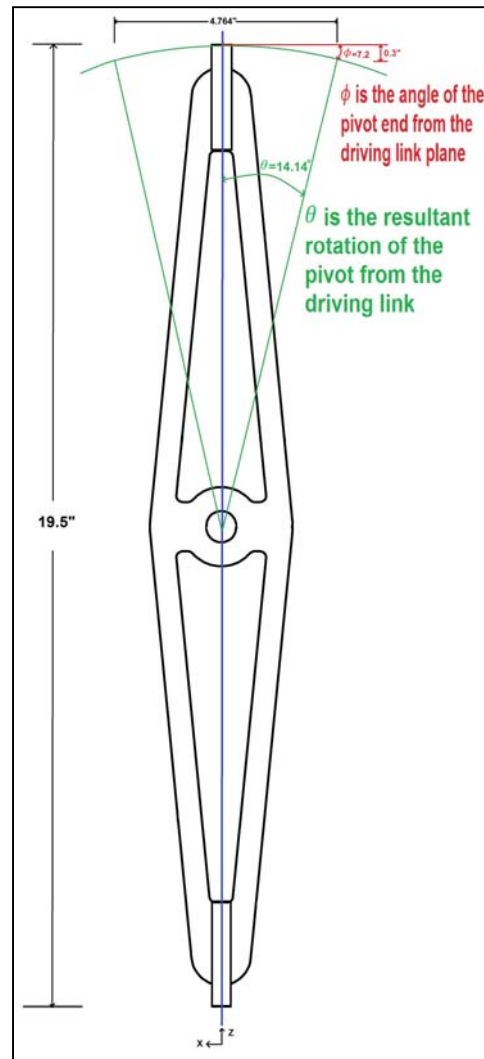


Figure 7: Differential Rod Pivot Link. The rod connecting the driving link attaches to the pivot link at the rectangular ends shown. This pivot link will take driving link rotation from one end and rotate about the central shaft moving the driving link for the other rocker an equal and opposite amount of rotation.

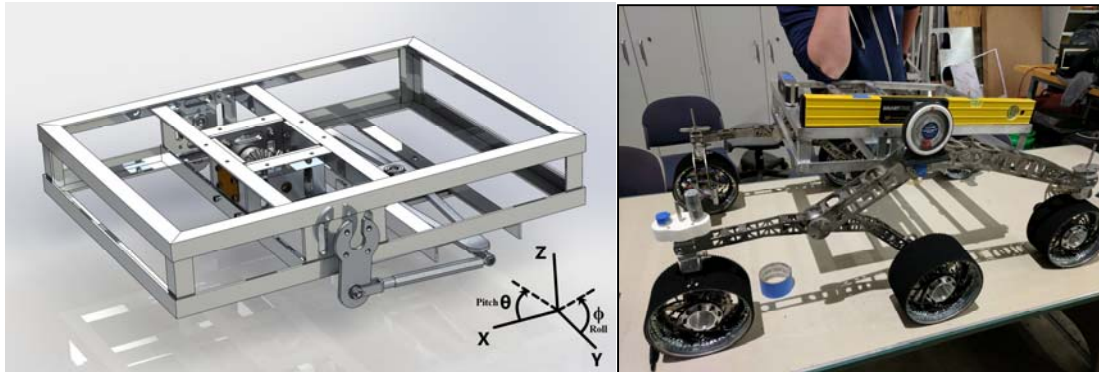


Figure 8: a) SolidWorks® render of the chassis with both differential options present. The orientation angles are defined via the coordinate axes shown. Rotation of the chassis is about the center point of the gearbox. b) Experimental test-setup on left suspension with measuring device placement for roll, pitch, pitch max, and pitch min angle collections. The magnetic protractor indicated the angle of rotation the rocker linkage was brought to for simulation of uneven terrain.

The rocker linkage was elevated at 10° increments up to 60° from the table plane measured with the magnetic protractor. Elevating the bogie to 60° resulted in the rocker linkage inclining to only 10° . If the bogie was elevated higher than 60° , with the size of the wheels and geometry of the bogie link, the middle wheel would eclipse the rotation point of the bogie making it impossible for the bogie to come back to the rest position. To keep whole and consistent inclination increments, the bogie was raised at increments that inclined the rocker at 2° per increment. This resulted in six measurement levels for rocker inclination and five levels for bogie inclination.



Figure 9: $\beta = 60^\circ$ inclination of the left suspension rocker linkage. This was the most extreme inclination capable of PicusMartius without the bogie driving the rocker linkage past perpendicular with the ground.

Fig. 9 shows the typical procedure where the left suspension rocker linkage was inclined to 60° . At each increment, both the pitch and the roll of the rover were recorded first. Additional force was applied at the end of the chassis to induce extra torque in both directions of pitch rotation. This allowed approximation of the maximum and minimum potential pitch angles at that given increment to use Eq. (6) to calculate delta. To provide at least 95% confidence in statistical analyses, the sample size was determined to be 20 measurements per increment for the pitch, roll, and delta using the equation for sample size needed for a specified confidence interval [6] with an estimated width of one degree and an expectation that the standard deviation of the measurements would not exceed one degree. The estimated calculation resulted in a sample size of 16 thus a sample size of 20 was used to compensate the estimations made in the sample size calculation.

Once the measurements were taken, the Angle Finder and magnetic protractor were attached to the top right of the chassis and right rocker linkage at the differential shaft, respectively, and the entire process was repeated for the right rocker-bogie mechanism. Collection of measurements for both rocker bogie sides at the various increments was performed for both the differential gearbox and the differential rod systems resulting in 78 comparative scenarios between the differential gearbox and the differential rod for a total of 3120 total measurements taken.

IV. RESULTS AND DISCUSSIONS

The analysis of the collected data is meant to show that one differential system performs better than the other. The pitch angle of the chassis (θ), the roll angle (ϕ), and delta pitch (Δ) are indicative of how well the differential system is performing at keeping the chassis level compared to expectations. The ideal values for each of the measurands are shown in Eq. (7), Eq. (8), and Eq. (9) where β in Eq. (8) is the inclination angle of the rocker linkage measured with the magnetic protractor.

$$\Delta_{ideal} = 0^\circ \tag{7}$$

$$\theta_{ideal} = \frac{\beta_{rocker\ 1} + \beta_{rocker\ 2}}{2} \tag{8}$$

$$\phi_{ideal} = 0^\circ \tag{9}$$

Because of the nature of the Rocker-Bogie suspension, the rocker linkage drives the differential which makes the pitch angle of the chassis half the sum of the inclination angles of the rocker linkages (parallel output rotation to output angle in kinematics of differential gear [7]). Given the nature of this data collection, one of the rocker linkages will have zero inclination at each measurement thus making the ideal value half the inclination angle of each incremental raise of the other rocker. In terms of the roll and the calculated delta, both would ideally be zero. The delta in the pitch should be kept to a minimum to reduce vibration risk and the roll should be kept to a minimum to reduce the chance of tipping during inclined travel. Comparison of performance between the systems will be accomplished by a derived metric described later in this paper. The sign convention used for measuring each of the angles with respect to the side of the chassis (F, R, and L, shown in Fig. 4 and Fig. 5) is shown in Fig. 10.

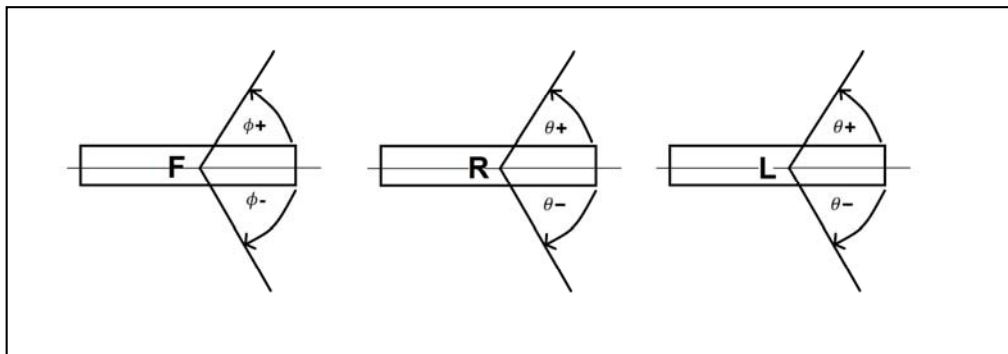


Figure 10: Roll angle (ϕ) and Pitch Angle (θ) sign convention based upon which suspension side was being tested. The delta (Δ), was a magnitude of a difference and thus was always considered positive.

To show significant differences between the systems, a two-sample pooled difference of means t-Test was conducted for each angle measurement at each rocker linkage inclination. For each system’s increment measurement set, the mean (μ) and standard deviation (s) of the sample were calculated and utilized to determine the test statistic t-value based on the difference between the differential gearbox’s mean and the differential rod’s mean. The resulting t-value is based on Eq. (10) [8]:

$$t_0 = \frac{\bar{x}_1 - \bar{x}_2 - \Delta_0}{s \sqrt{\frac{1}{n_1} + \frac{1}{n_2}}} \tag{10}$$

The Δ_0 term indicates the desired difference between the two systems and thus the resulting difference of the means in the null hypothesis (H_0) of the t-test shown in Eq. (11):

$$H_0: \mu_1 - \mu_2 = \Delta_0 \tag{11}$$



In this example, the objective of the null hypothesis is to exemplify that there is no difference in performance between the two differential systems, meaning the mean of each system’s increment measurements are the same, resulting in a Δ_0 value of 0. The alternate hypothesis that is being tested is to indicate that the difference between the means does not equal the Δ_0 term at all shown in Eq. (12):

$$H_A: \mu_1 - \mu_2 \neq 0 \tag{12}$$

The s_p term is the pooled estimator of the variance of the mean differences. The s_p term is a weighted average of the standard deviations of the data collected shown in Eq. (13) [8]:

$$s_p = \sqrt{\frac{(n_1-1)s_1^2 + (n_2-1)s_2^2}{n_1+n_2-2}} \tag{13}$$

The variance of the data collected for each system (s_1^2 and s_2^2) included the design stage uncertainty of the instruments used to measure the angles. The design stage uncertainty of a measurand is shown in Eq. (14) [9]:

$$U_d = \sqrt{U_0^2 + \sum_{i=1}^{n_i} U_{I_i}^2} \tag{14}$$

$U_0 =$ Zero-Order Uncertainty equal to one-half the instrument resolution

$U_I =$ Instrument uncertainty resulting from the summation of the squares of the instrument’s elemental errors

The design stage uncertainty calculated for the Smart Level Angle Finder used to measure the pitch and the resulted calculated delta values was $\pm 0.05^\circ$. The design stage uncertainty calculated for the Mitutoyo digital protractor used to measure the roll angle was $\pm 0.25^\circ$. The calculated uncertainties were added to their respective variances used in Eq. (13) after data collection to incorporate the measurement uncertainty into the pooled estimator of variance. The resulting standard deviation was then used to compute the standard six-sigma natural limits of the measurements.

Since the sample size of increment was equal for both systems, $n_1 = n_2$ which reduced the resulting t-value in Eq. (10) down to Eq. (15):

$$t_0 = \frac{\bar{x}_1 - \bar{x}_2}{s_p \sqrt{\frac{2}{n}}} \tag{15}$$

Determining if the alternate hypothesis supports rejection of the null hypothesis comes from a fixed significance level rejection criterion. A two-sided alternate hypothesis, as in this case, is as follows:

$$\text{Reject if: } t_0 < -t_{\alpha/2, n_1+n_2-2} \text{ or } t_0 > t_{\alpha/2, n_1+n_2-2}$$

To maximize certainty of a statistically significant performance difference, every t-value was calculated at 99% confidence level making the fixed significance level rejection criterion value $\alpha = 0.01$. This made the reference t-values for rejection of the null hypothesis from the cumulative t-distribution table [8]:

$$\text{Reject if: } t_0 < -2.712 \text{ or } t_0 > 2.712$$

Thus, if the resulting t-value calculated from the difference between the two means satisfies the rejection criteria, there is a statistically significant difference in the results from one differential system to the other at that measurement.

Table 2 shows the calculated t-values generated from the different measurands. Any measurand that is underlined and italicized shows a statistically significant difference in the values collected for the gearbox and rod system. The table shows that for both the pitch angle and pitch delta measurements, there was a statistically significant difference for all increments. This was not the case for the roll angle, as the only measurands that showed statistically significant differences were at 8° for the right bogie, 40° and 60° for the right and left rocker and 50° for the left rocker. Fig. 11 shows a graphical representation of the t-values calculated for the roll angle measurements. A statistically significant difference in the



measurand is when a value lies outside the marked null hypothesis acceptance region. While the systems started to present statistically significant differences in measurements with $\beta > 30^\circ$, majority of the roll angle measurands did not present a significant difference in the recorded values enough to allow for a definitive comparison of just the roll angle.

Table 2: Resulting test statistic t-values between the Differential Gearbox and Rod systems. Values that indicate significant performance difference at 99% confidence are underlined and italicized. Note that 20 of the 26 roll angle comparisons did not show a statistically significant difference in the data collected.

Bogie (L) β	0°	2°	4°	6°	8°	10°	
Delta Δ	<u>66.1</u>	<u>74.35</u>	<u>67.34</u>	<u>74.67</u>	<u>64.93</u>	<u>61.09</u>	
Pitch θ	<u>-66.14</u>	<u>-52.06</u>	<u>-69.57</u>	<u>-65.27</u>	<u>-47.49</u>	<u>-53.84</u>	
Roll ϕ	1.56	-0.52	1.61	0.21	-1.21	-2.1	
Bogie (R) β	0°	2°	4°	6°	8°	10°	
Delta Δ	<u>73.29</u>	<u>75.91</u>	<u>72.11</u>	<u>64.98</u>	<u>49.29</u>	<u>70.74</u>	
Pitch θ	<u>67.82</u>	<u>79.91</u>	<u>80.35</u>	<u>59.98</u>	<u>60.88</u>	<u>71.07</u>	
Roll ϕ	1.24	-1.91	-2.35	-1.47	<u>-3.02</u>	0.2	
Rocker (L) β	0°	10°	20°	30°	40°	50°	60°
Delta Δ	<u>44.07</u>	<u>44.38</u>	<u>68.18</u>	<u>61.61</u>	<u>47.16</u>	<u>43.57</u>	<u>41.6</u>
Pitch θ	<u>-61.1</u>	<u>-46.66</u>	<u>-24.85</u>	<u>-21.01</u>	<u>-28.36</u>	<u>-37.2</u>	<u>-25.13</u>
Roll ϕ	0.72	0.52	0.26	0.17	<u>-4.12</u>	<u>-7.26</u>	<u>-6.64</u>
Rocker (R) β	0°	10°	20°	30°	40°	50°	60°
Delta Δ	<u>66.26</u>	<u>72.43</u>	<u>65.36</u>	<u>72.94</u>	<u>44.93</u>	<u>76.66</u>	<u>46.28</u>
Pitch θ	<u>86.72</u>	<u>62.67</u>	<u>44.01</u>	<u>55.28</u>	<u>34.03</u>	<u>48.46</u>	<u>28.37</u>
Roll ϕ	0.94	1.79	0.78	2.32	<u>4.16</u>	2.7	<u>2.85</u>

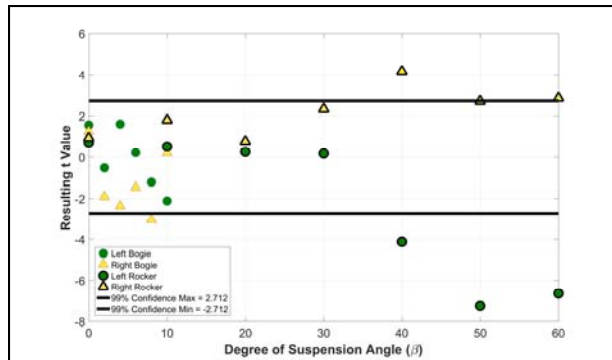


Figure 11: Difference of means two-sided t-Test values between the left and right rocker and bogie roll angle measurements. To have a statistically significant difference in values to allow for a definite comparison, the t-value should lie outside the null hypothesis acceptance region marked by the confidence max and min values of ± 2.712 . Majority of the values lie within the null hypothesis acceptance region thus a direct performance comparison of just the roll angle would not be reasonable.

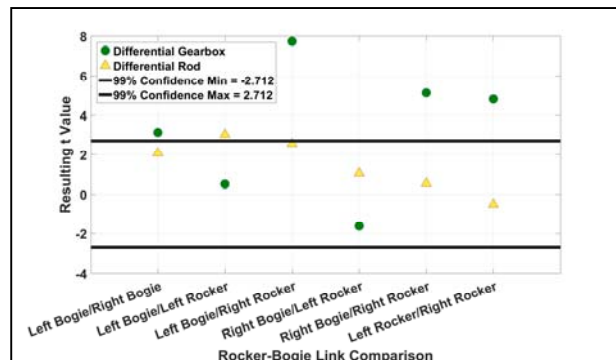


Figure 12: Difference of means two-sided t-test values for the calculated Δ between each linkage at $\beta = 0$. Theoretically, this data should be able to be combined given all is when the system is at rest, but the data indicates significant enough differences between the data sets at certain measurands to prevent a combination of all the data points into one set at $\beta = 0$.

Both the left and right rocker-bogie systems were measured at a resting angle of $\beta = 0^\circ$ or in other words, “the system at rest.” It could be assumed that all the $\beta = 0^\circ$ data could be combined into one large data set for comparison between the two systems at rest.

Upon further investigation, Fig. 12 shows that there was a significant enough difference in the delta calculation at rest for the measurements taken when moving each part of the rocker-bogie that prevented combining all the $\beta = 0^\circ$ inclination angle data together for each system. Thus, analysis of the data required separate comparisons between the left and right rocker and bogie data sets for $\beta = 0^\circ$ indicative in Fig. 13, Fig. 14, and Fig. 15 where the data on the left side of each chart up through the “0B” increment indicates measurements when raising the bogie linkage and the data on the right side of the chart from “0R” to the end indicates measurements when raising the rocker linkage. All data associated with the gearbox is indicated in green while all data associated with the rod system is indicated in yellow. The respective left and right rocker-bogie linkages are distinguished by the left linkage data being outlined and at each measurement the outlined left bars being the left most bars.

Fig. 13 indicates that the differential gearbox was on average 5.01° off the ideal pitch angle while the differential rod system was on average 0.66° off the ideal. The differential gearbox was on average 7.64 times farther from the ideal pitch than the differential rod system. This indicates the differential rod system performs closer to expectations in terms of pitch angle.

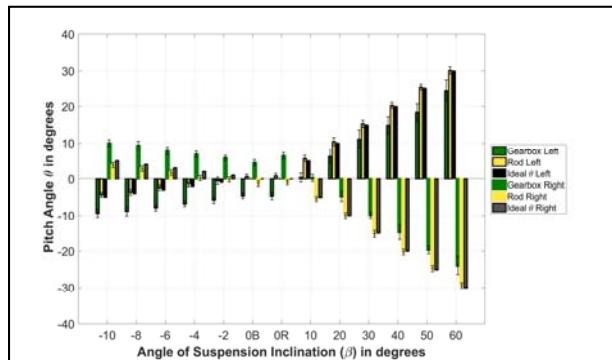


Figure 13: Resulting pitch angle measurements from inclining the bogie and rocker linkages for each respective differential system compared to the ideal at each inclination angle.

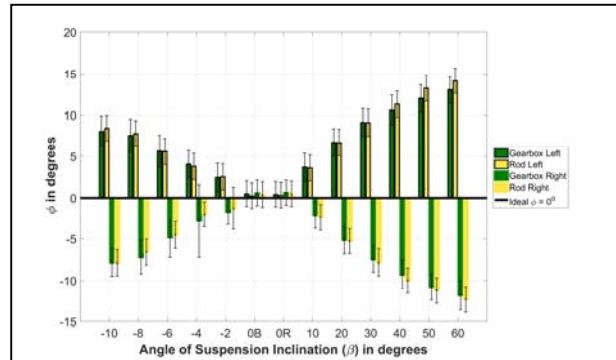


Figure 14: Resulting roll angle measurements from inclining the bogie and rocker linkages for each respective differential system compared to the ideal at each inclination angle. Note that a direct comparison between the two differential systems with just the roll angle would not be statistically significant as discussed prior.

Fig. 14 indicates the differential gearbox was on average 5.99° off the ideal roll angle while the differential rod system was on average 6.10° off the ideal. The differential rod system was on average 1.02 times farther from the ideal than the differential gearbox. This value would suggest that the differential rod and differential gearbox systems were almost equal in terms of degrees off the ideal roll angle with the differential gearbox being slightly closer to expectations. However, earlier it was determined that the data collected for the roll angles of each system did not have a statistically significant enough difference to allow a direct comparison. This is supported with how close the average degree off was for each system. Thus, a definitive choice of a system performing closer to expectations in terms of the roll angle alone cannot be given.

Fig. 15 indicates the differential gearbox was on average 7.20° off the ideal delta magnitude while the differential rod system was on average 0.70° off the ideal. The differential gearbox was on average 10.24 times farther from the ideal than the differential rod system. This indicates the differential rod system performs an order of magnitude closer to expectations in terms of the delta.

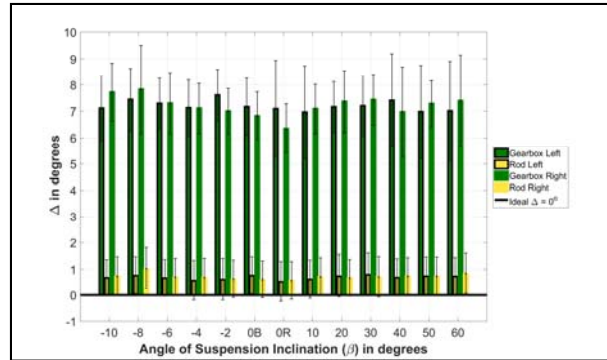


Figure 15: Resulting delta measurements from inclining the bogie and rocker linkages for each respective differential system at each inclination angle.

V. THE PICUS NUMBER, P_m

Even though in the previous figures there appears to be distinct performance differences between the two systems with the differential rod performing closer to expectations, there still was a need for a quantitative representation of a performance metric. The Picus Number (P_m) was developed to have one dimensionless metric to describe the resulting performance of a Rocker-Bogie differential system. The Picus Number is generated through the summations of the difference between the calculated mean at an inclination angle and the expected value for the different measurands. This difference was then multiplied by the standard deviation of the measurand to incorporate the variance in the data collection. This result was taken as an absolute value to negate negative values from sign conventions. The resulting values for all the measurands are then multiplied by a gain which weights the angle measurements subjectively more important to the overall performance. The units of this gain value are considered the subjective weight of the measurement per degree squared ($\frac{weight}{deg^2}$) analogous to how pressure is a force applied to an area but in this case the subjective weight of importance is the force. The result is then divided by the total number of measurands for each system creating a dimensionless metric shown by Eq. (16).

$$P_m = \frac{k_\Delta}{n} \sum_{i=1}^n (\bar{\Delta}_i - \Delta_{ideal,i}) s_{\Delta,i} + \frac{k_\theta}{n} \sum_{i=1}^n |(\bar{\theta}_i - \theta_{ideal,i}) s_{\theta,i}| + \frac{k_\phi}{n} \sum_{i=1}^n |(\bar{\phi}_i - \phi_{ideal,i}) s_{\phi,i}| \quad (16)$$

- n = Number of inclination angles tested
- k_Δ = Weighted gain for play in the pitch
- k_θ = Weighted gain for pitch angle
- k_ϕ = Weighted gain for roll angle
- s_i = Measurement Standard Deviation
- $\bar{\Delta}$ = Average play in pitch at designated inclination
- Δ_{ideal} = Ideal play in pitch
- $\bar{\theta}$ = Average pitch angle at designated inclination
- θ_{ideal} = Ideal pitch angle at designated inclination
- $\bar{\phi}$ = Average roll angle at designated inclination
- ϕ_{ideal} = Ideal roll angle at designated inclination

The gain values associated with each measurand were based upon a percentage of importance determined by opinion of the qualitative features of the system. It was decided to split up the gains as follows: $k_\Delta = 0.5$, $k_\theta = 0.2$, and $k_\phi = 0.3$. The delta received the highest weight of importance because during operation, high amplitude cyclic motion of the chassis can cause enough vibration to jar electrical components and/or produce enough wear on certain mechanical components to drastically lower the life expectancy of the part. The roll angle and the pitch angle were of close to the same importance



simply because both affect how level the chassis is during operation, but it was decided to place slightly more weight on the roll angle due to the rotation the differential system experiences from the roll. The pitch angle rotates about the main differential shaft and thus if only the pitch was changing, the differential would essentially be acting as a driving mechanism for chassis rotation. Since the roll creates a rotation about an axis perpendicular to the differential shaft, this would create irregular forms of static loading. With irregular static loading, the ability to predict failure becomes increasingly difficult driving the decision to weigh the roll angle difference higher than the pitch angle.

Incorporating the subjective gains and ideal values reduces the Picus Number performance metric equation to Eq. (17).

$$P_m = \frac{0.5}{n} \sum_{i=1}^n \bar{\Delta}_i s_{\Delta,i} + \frac{0.2}{n} \sum_{i=1}^n |(\bar{\theta}_i - \theta_{i,ideal,i}) s_{\theta,i}| + \frac{0.3}{n} \sum_{i=1}^n |\bar{\phi}_i s_{\phi,i}| \quad (17)$$

The idealized Picus Number would be $P_m = 0$ indicating that the differences between the collected data and the idealized values are zero, but this is physically impossible to achieve due to manufacturing tolerances and uncertainties in data collection. Therefore, Picus Numbers that are closer to zero indicate a better performing system. Since there were thirteen measurands for each side of the suspension, the total number of measurands used in calculating the Picus Number was 26 ($n = 26$). The resulting Picus Numbers for the two differential systems are:

$$P_{m, Gearbox} = 4.45$$

$$P_{m, Rod} = 1.65$$

From Fig. 13 and Fig. 15 there is some indication that the differential rod performed better than the differential gearbox at the respective measurement expectations, but now the Picus Number is able to quantitatively show with statistical significance the performance difference. The differential rod performs closer to theoretical expectations as its Picus Number is closer to zero than the differential gearbox. In terms of the Picus Number, the design and fabrication of the differential rod system performed 2.7 times better than the design and fabrication of the differential gearbox system.

VI. CONCLUSION

Prior research had shown the impact the differential system can have on the roll and pitch of a rover implementing a Rocker-Bogie suspension system. However, design decisions were not justified by any quantitative comparison between differential types. This led to the creation of the Picus Number to allow for a way to definitively compare Rocker-Bogie differential system designs. Using the Picus Numbers generated for the two differential system designs used in this experiment on the NIU Mars Rover Team's rover, PicusMartius, it was clear to implement the differential rod system into the overall rover design because of its indication of performing 2.7 times better than the differential gearbox system.

From direct observation of the two designs, it is apparent that gear driven systems are adversely affected by the backlash that exists between gears. Because it is impossible to create a perfect gear mate, there will automatically be some space for slight movement between the gear teeth due to tolerances and manufacturing limitations. In addition, the gearbox that houses the differential system would need to be structurally robust with precise axes locations to limit the amount of play at the gear mates. The success of the differential rod system is likely due to the ability to create secure joints between the linkages with rotation compensation via the rod ends and swivel bearings.

It is important to note that the Picus Number is design specific and now, there is not a standard to compare to for satisfactory designs. The reason there was a comparison in this study was because it was a direct comparison between one system and another. It appears that effective joining methods of the differential linkages or gear mates are pivotal to reducing the overall Picus Number of the system, and thus increasing the Rocker-Bogie suspension performance. If more teams utilizing a Rocker-Bogie suspension would replicate this experiment and determine the Picus Number for their respective design, a "Standard Picus Number" can be developed for reference by teams during the development stage of their Mars rovers. The standard Picus Number would be a comparison value to achieve through design and fabrication and would indicate to a team that their design will perform adequately.

VII. ACKNOWLEDGEMENTS



The NIU Mars Rover team appreciates the NIU Office of Student Engagement and Experiential Learning for providing the Undergraduate Special Opportunities in Artistry and Research (USOAR) Grant to support the work.

REFERENCES

- [1] Howell, E., "A Brief History of Mars Missions," Last modified April 08, 2019. <http://www.space.com/13558-historic-mars-missions.html>
- [2] National Aeronautics and Space Administration, "Wheels and Legs," Mars Curiosity Rover, Accessed January 5, 2020. <https://mars.nasa.gov/msl/spacecraft/rover/wheels/>
- [3] The Mechanic, "Differential (mechanical device)," Accessed January 5, 2020. <http://themicanic.weebly.com/uploads/4/3/5/7/4357357/differentials.pdf>
- [4] Nguyen, C., DuCharme, L., et al., "Astro the Rover: Mars Rover Development and Design," California State University Fullerton, December 22, 2014. <http://www.fullerton.edu/titanrover/project/documentation/FinalReport.pdf>
- [5] Budynas, R. G., and Nisbett, J. K., *Shigley's Mechanical Design*, 10th ed., New York City, NY: McGraw-Hill Education, 2015.
- [6] Devore, J. L., *Probability and Statistics for Engineering and the Sciences*, 8th ed., Mason, OH: Cengage Learning, 2011.
- [7] Koseki, Y., and Chinzei, K., "'Differential Gear Transmission for Low-Speed Drive of Ultrasonic Motor," *3rd Asian Conference on Computer Aided Surgery*, Singapore, 2007.
- [8] Montgomery, D. C., *Introduction to Statistical Quality Control*, 7th ed., Hoboken, NJ: John Wiley & Sons, 2013.
- [9] Dunn, P. F., *Measurements and Data analysis for Engineering and Science*, 3rd ed., Boca Raton, FL: Taylor & Francis Group, 2014.
- [10] McMaster Carr, "Gears and Speed-Reducing Worm Gears," Accessed January 4, 2020. <https://www.mcmaster.com/#catalog/123/1121/=17a9dit>